# Diesel exhaust nanoparticles and their behaviour in the atmosphere

Harrison, Roy M.; Mackenzie, Angus; Xu, Hongming; Alam, Mohammed S.; Nikolova, Irina; Zhong, Jian; Singh, Ajit; Zeraati-Rezaei, Soheil; Stark, Christopher; Beddows, David C.S.; Liang, Zhirong; Xu, Ruixin; Cai, Xiaoming

*DOI:*
10.1098/rspa.2018.0492

# DIESEL EXHAUST NANOPARTICLES AND THEIR BEHAVIOUR IN THE ATMOSPHERE

**Roy M. Harrison[1,2*†], A. Rob MacKenzie[1,3], Hongming Xu[4], Mohammed S. Alam[1], Irina Nikolova[1], Jian Zhong[1], Ajit Singh[1], Soheil Zeraati-Rezaei[4], Christopher Stark[1], David C.S. Beddows[1,2], Zhirong Liang[5] and Ruixin Xu[1], Xiaoming Cai[1]**

**[1]School of Geography, Earth and Environmental Sciences and**
**[2]National Centre for Atmospheric Science**
**University of Birmingham**
**Edgbaston, Birmingham B15 2TT, UK**

**[3]Birmingham Institute of Forest Research, University of Birmingham, Edgbaston, Birmingham, B15 2TT, UK**

**[4]Department of Mechanical Engineering**
**School of Engineering, University of Birmingham, Edgbaston**
**Birmingham, B15 2TT, UK**

**[5]School of Energy and Power Engineering**
**Beihang University, Beijing, 100191, China**

**Running Head: Behaviour of Diesel Exhaust Particles**

[*] To whom correspondence should be addressed.
Tele: +44 121 414 3494; Fax: +44 121 414 3709; Email: r.m.harrison@bham.ac.uk

[†]Also at: Department of Environmental Sciences / Center of Excellence in Environmental Studies, King Abdulaziz University, PO Box 80203, Jeddah, 21589, Saudi Arabia

**ABSTRACT**

Diesel engine emissions are by far the largest source of nanoparticles in many urban atmospheres, in which they dominate the particle number count, and may present a significant threat to public health. This paper reviews knowledge of the composition and atmospheric properties of diesel exhaust particles, and exemplifies research in this field through a description of the FASTER project (Fundamental Studies of the Sources, Properties and Environmental Behaviour of Exhaust Nanoparticles from Road Vehicles) which studied the size distribution — and, in unprecedented detail, the chemical composition — of nanoparticles sampled from diesel engine exhaust. This information has been systematised and used to inform the development of computational modules that simulate the behaviour of the largely semi-volatile content of the nucleation mode particles, including consequent effects on the particle size distribution, under typical atmospheric conditions. Large-eddy model studies have informed a simpler characterisation of flow around the urban built environment, and include aerosol processes. This modelling and engine-lab work has been complemented by laboratory measurements of vapour pressures, and the execution of two field measurement campaigns in London. The result is a more robust description of the dynamical behaviour on the sub-km scale of diesel exhaust nanoparticles and their importance as an urban air pollutant.

**Keywords:** Diesel exhaust; Particulate matter; Evaporation; Hydrocarbons; Aerosol dynamics

## INTRODUCTION

Airborne particulate matter is the pollutant currently believed, on the basis of epidemiological research, to have the greatest impact upon public health. In the latest analysis of data from the Global Burden of Diseases Study, ambient particulate matter pollution ranked fifth as an avoidable cause of death and sixth as a contributor to disability-adjusted life years lost [1]. In 2015, exposure to particulate matter expressed as $PM_{2.5}$ caused 4.2 million deaths and 103.1 million disability-adjusted life years (DALYs) lost, representing 7.6% of total global deaths and 4.2% of global DALYs. This was an increase in both relative to 1990. Although most of the quantitative information on health effects is based on the $PM_{2.5}$ metric, which describes the mass concentrations of particles of 2.5 micrometres or smaller in the air, the airborne particles extend over a much wider size range. Particles newly formed from gas-to-particle conversion processes are around 1 nanometre in diameter while the largest particles with a significant lifetime in the atmosphere are of the order of 100 micrometres diameter [2]. Thus, airborne particles cover five orders of magnitude in size (and fifteen orders of magnitude in mass) but are also hugely diverse chemically. Although it might reasonably be expected that particle toxicity would be profoundly influenced by particle size and chemical composition (which would be expected to determine individual particle toxicity), there is no clear consensus upon which size fractions or chemical components present the greatest toxicity, and the literature surrounding this issue does not paint a consistent picture [3,4].

Ultrafine particles (UFP, with particle diameter Dp < 100 nm) are emitted into outdoor urban air predominantly by road traffic, particularly diesel exhaust [5, 6]. UFP from traffic are often released close to members of the public, and research has accumulated pointing to the toxicity and potentially harmful effects of UFP on human health [7]. The other main source of nanoparticles in the atmosphere is regional nucleation in which new particles form from oxidation of gases. This is less important than direct particle emissions in urban areas of northern Europe [8,9].

Research on airborne particulate matter involves many aspects (see Figure 1), from particle emissions, through near-field dispersion, chemical and physical transformations in the atmosphere, characterisation of airborne particles, measurement and modelling of personal exposure, and the study of effects on human health. This article uses one specific project which has involved an in-depth study of the size distribution and chemical composition of particles emitted by diesel engines and the measurement and modelling of their behaviour in the atmosphere to illustrate the latest research conducted in this field. Diesel particles well exemplify the challenges of studying semi-volatile airborne particles. Their sizes run from a few nanometres to a few hundred nanometres and their composition varies with size, as indicated in the following. The particles smaller than around 30 nanometres diameter comprise predominantly high molecular weight hydrocarbons which derive from unburnt fuel and lubricating oil [10]. These are formed as the exhaust gases mix with cooler ambient air [11], and condensation appears to take place on nanometre-sized nuclei of metallic ash or sulphuric acid [12, 13]. The larger particles comprise mainly graphitic elemental carbon in loose chain aggregates onto which are condensed high molecular weight hydrocarbons [14]. The hydrocarbon compounds, which comprise a substantial proportion of particle mass [15] and range from around $C_{12}$ to > $C_{36}$ are semi-volatile, which means that they partition between the condensed phase and the vapour phase in a way which is affected by their vapour pressure, the ambient temperature, the particle composition and size, and the concentration of the vapour phase surrounding the particle. The effect of temperature is seen in seasonal effects upon particle number [16] and size distributions [17] in urban air. The introduction of diesel particle filters (DPF) is changing the nature of diesel particles, but there have been few detailed measurements to date, and emissions from pre-DPF vehicles probably dominate atmospheric diesel particles.

**Dynamics of Airborne Particles**

Airborne particles are subject to a number of dynamical processes which influence both their size distribution and airborne concentration, and size distributions downwind of a busy road show complex behaviour [18, 19, 20]. Relevant processes include the following:

*Coagulation.* As particles move through the air, they are subject to collisions which generally lead to coalescence, referred to as coagulation. This is a process which is strongly dependent on the number concentration of particles and leads to a decrease in particle number concentration, but an increase in average size. It is not generally a very rapid process in the atmosphere as the number concentrations of particles are not sufficiently high, but does cause a ~ 5% reduction in diesel UFP numbers dispersed throughout a street canyon [21].

*Deposition*. Particles are removed from the atmosphere by deposition to surfaces. Those of larger size, greater than about 5 μm diameter, have significant gravitational settling velocities and this, together with scavenging by clouds and rain, are the main removal mechanisms. Smaller particles, and especially those below 100 nm diameter, are subject to Brownian diffusion and tend to be subject to diffusive deposition to surfaces. We find a ~ 3% effect on diesel UFP emissions from deposition dispersed throughout a street canyon [21].

*Condensational growth*. The atmosphere is an oxidising environment and there is a constant conversion of vapour phase molecules to more oxidised forms which unless fragmented have a strong tendency to condense. Under most circumstances it is energetically most favourable for them to condense onto existing particle surfaces hence causing a growth of particles without a change in number concentration. Gas-to-particle mass exchange is always in principle two-way, responding to the difference between the ambient partial pressure of a gas and its saturation vapour pressure in the particle phase [22].

*Evaporation*. Particles comprised of semi-volatile materials are those with saturation vapour pressures equivalent to concentrations between approximately $10^{-1}$ to $10^{4}$ μg $m^{-3}$ and are liable to evaporate in circumstances where the vapour phase concentrations fall below equilibrium saturation vapour pressures for individual compounds in the mixture [23]. This leads to particle shrinkage and a change in particle composition for multi-component particles, but not a change in number concentration [24, 25], unless particles evaporate fully. Heating diesel particles shows a substantial volatile fraction [26, 27, 28].

*Chemical reaction*. Most particles comprising organic matter contain some potentially reactive molecules. In most cases, reactions in the condensed phase are relatively slow due to the need for transfer of oxidant species from the gas phase into the particle. Exceptions include compounds such as oleic acid which contain an olefinic double bond which reacts with ozone, an oxidant present in the atmosphere at much higher concentrations than most other oxidant species [29]. Theoretical considerations indicate that for most semi-volatile molecules, reactions of the vapour phase component tend to dominate over condensed phase reaction processes [30]. This adds considerable complications in predicting the behaviour and atmospheric lifetime of these compounds. Research in London has shown that diesel-related hydrocarbons can dominate gas phase reactive carbon [31] and that the intermediate-volatility organic compounds (approx. $C_{12}$-$C_{22}$) emitted largely by diesels can contribute ~30% of the annual average secondary organic aerosol around London [32]. This is, however, likely to change with an increased penetration of vehicles with aftertreatment [33].

**The FASTER Project of Diesel Particles Emissions and their Atmospheric Behaviour**

Figure 2 exemplifies the processes of how semi-volatile diesel particles form as hot exhaust cools on mixing with ambient air [10, 11] and how the particles can subsequently evaporate as they are diluted on moving away from source. It also includes an important process in which the vapours are then

oxidised forming secondary particles of greater mass, a paradigm proposed by Robinson et al. [34, 35, 36, 37, 38].

The FASTER project (Fundamental Studies of the Sources, Properties and Environmental Behaviour of Exhaust Nanoparticles from Road Vehicles) comprises four main science topics shown in Figure 3. These topics will be described in turn and illustrated with examples of some of the key findings. Figure 3 also shows the intermediate objectives which summarise the underlying rationale for the science topics, and the final objectives which have both scientific and policy relevance.

**Science Topic 1: Characterisation of Emissions**

Most studies of diesel particle emissions depend upon use of a vehicle run on a chassis dynamometer [39, 40], on the road [41, 42] or an engine alone operated on an engine dynamometer [27]. In the FASTER project, diesel particle emissions were sampled from test engines run under typical operating conditions on an engine dynamometer in the laboratory, and the emitted particles were diluted with clean air before collection so as to simulate atmospheric dilution. Details of the engine testing system and sampling system are given by Alam et al. [43], and a schematic of the engine test cell appears in Figure S1. This allowed sampling of engine-out exhaust, and exhaust after passing through a diesel oxidation catalyst (DOC), and a DOC and diesel particulate filter (DPF) in series. It was important to make measurements both on raw exhaust and after the control devices, as the current European diesel vehicle fleet contains vehicles both with and without DPF [44], and in many countries DPF cannot be used due to an inadequate fuel quality [45]. Dilution of the emissions is important, as firstly it prevents condensation of water as the cooling exhaust gases supersaturate, and secondly, it controls the particle size distribution by determining whether semi-volatile vapours condense upon larger carbonaceous particles or upon smaller nuclei of sulphuric acid or trace metals causing them to grow [10]. Consequently, it can also affect the mass of particles emitted [46, 47, 48].

The particles were size-fractionated during collection and transferred to the analytical laboratory where their composition was determined by the advanced technique of 2-dimensional gas chromatography with detection by time-of-flight mass spectrometry GCxGC-ToFMS [49]. The use of an advanced separation technique is essential as traditional 1-dimensional gas chromatography will only separate around 10% of the mass of the volatile component of the particles whereas the 2-dimensional technique can give a virtually complete separation of thousands of individual compounds.

In two-dimensional gas chromatography, compounds are first separated in a conventional manner on a chromatographic column according to their volatility. Column effluent is condensed, and every few seconds is re-evaporated and passed through a short second chromatographic column which separates on the basis of polarity. Hence, a two-dimensional chromatogram is developed, as shown in Figure S2. This gives excellent separation of individual compounds which can be characterised on the basis of their mass spectra. The groups of compounds which were analysed in diesel exhaust (particulate and gaseous), diesel fuel, engine lubricating oil and ambient air appear in Table 1. During the course of the work, a modification to the mass spectrometer was installed which allowed electron ionisation at energies as low as 10eV, as well as the conventional 70eV to be used during detection. This lower ionisation energy allowed the observation of molecular ions and much larger fragment ions than are typically seen in the 70eV mass spectra, allowing the identification of a much wider range of compounds [49, 50]. By this method, about 90% mass closure can be achieved [51].

A typical profile of n- and iso-alkane concentrations in diesel engine exhaust is shown for the vapour phase and condensed (particulate) phase in Figure 4. This shows a peak abundance of particle-phase alkanes at $C_{25}$, which is fairly typical of diesel exhaust. As anticipated, the vapour form dominates the alkanes at lower molecular weights, with the particle phase dominant above around $C_{20}$. Separate analyses of diesel fuel and lubricating oil suggest that unburnt fuel is largely responsible for the

alkanes $<C_{20}$, and lubricating oil for those $>C_{20}$. Generic speciation of compounds in diesel exhaust, diesel fuel and lubricating oil provides the basis for such a conclusion [51, 52]. Other such apportionment estimates have been reported [28, 53, 54,], and between diesel and gasoline emissions [37].

Particle number size distributions were also measured in the diluted engine exhaust and are exemplified by Figure 5 for low engine load. This shows a mode in the diluted raw exhaust (before DOC) at around 40 nm, with a shoulder seen just below 20 nm. The relative sizes of these modes are mainly sensitive to the engine operating conditions and dilution ratio, and the size distributions measured in roadside air (see later) give the greater emphasis to a mode at 20-30 nm which is responsible for the shoulder close to 20 nm in Figure 5. The mode at 40 nm, which is less prominent in the roadside data, is attributed to solid graphitic carbon-based "soot" particles, while the smaller mode comprises particles predominantly composed of condensed hydrocarbons [14, 55]. Figure 5 also shows the small effect of the DOC on the particle concentration and size distribution. The effect of the DOC is to remove some of the hydrocarbon vapour component of the exhaust aerosol, leading to evaporation of some of the SVOC content from the condensed phase material, hence effecting a reduction primarily in the smaller particles which have a higher SVOC content. Particle concentrations after the DPF are reduced to almost zero (filtration efficiency >99.95%) under steady state operating conditions, although other research has shown increased particle emissions during transient operating cycles [56, 57], and especially during DPF regeneration cycles [58, 59].

**Science Topic 2: Laboratory Studies**

In order to model the atmospheric behaviour of the semi-volatile hydrocarbons, it is necessary to specify their chemical composition, determined above in the analytical studies, their phase partitioning and the size distribution of the particulate fraction, determined in the engine laboratory, and the vapour pressures of the constituent molecules. A search of the literature revealed many past studies of the vapour pressures of the n-alkanes and it is also possible to calculate vapour pressures

based upon structure-activity relationships using the US EPA programme EPISUITE [as in 60] or the University of Manchester UManSysProp online tool [61]. The literature values of vapour pressure were mainly estimated from extrapolation of vapour pressures measured at higher temperatures, and although divergences were relatively small for the lower molecular weight compounds, literature values for the higher molecular weight compounds could vary by more than five orders of magnitude for a single compound. With such a wide range of values, the evaporative behaviour of the particles could vary greatly in rate according to which set of vapour pressures was adopted. Consequently, it was important to make new measurements of vapour pressures at close to ambient temperatures. Individual pure SVOC compounds were coated onto glass beads; microscopy revealed the liquid coating to be present as a super-cooled liquid (which has higher saturation vapour pressure than the more thermodynamically stable, but presumably kinetically hindered, crystalline solid). The coated beads were then packed into a temperature-controlled U-tube through which a gentle flow of nitrogen was passed, following the method of Verevkin et al. [62]. The nitrogen flow was set such that contact time with the coated beads was long enough to allow the vapour to equilibrate with the pure liquid phase, after which the saturated vapour was stripped out of the nitrogen gas flow in an adsorption tube and analysed using the GCxGC-ToFMS system. This technique gave repeatable measurements and vapour pressures intermediate between the highest and lowest values available from the literature, suggesting that the literature data were subject to random error, exacerbated by the large temperature extrapolation, rather than systematic bias.

**Science Topic 3: Field Measurements**

In parallel with the studies in the engine laboratory, measurements were made in central London (UK) of particles emitted on busy Marylebone Road (daily traffic flow ~ 80,000-90,000 vehicles) and transported subsequently by the wind into adjacent Regent's Park. Multi-site measurement campaigns were used to quantify the rate at which the particles change in size and composition during advection (horizontal transport) from the highway to the cleaner environment of the park [63].

Measurements of particle size distributions were made using scanning mobility particle sizers (SMPS) at five sites in all. Three sites were established especially for this project: Westminster University, sited on the roof overlooking the ground level Marylebone Road monitoring station; Regents University, on the roof of a building within Regents Park and 380 metres north of the Westminster University site; aloft at 160 metres above ground level on the BT Tower at a distance of 380 metres from the Marylebone Road site (see Figure S3). Data from these sampling sites was supplemented with data collected as part of a small national measurement network using two sampling sites: Marylebone Road, a kerbside site within a busy street canyon on the south of the highway directly below the Westminster University sampling site; and North Kensington, which is a central London background location without substantial local traffic activity located 4 km from the Marylebone Road site. Also located at the sampling stations were condensation particle counters which measure the total number of airborne particles above a lower cut point of around 3 nanometers diameter, and aethalometers which measure the black (elemental) carbon content of airborne particles, which in London is an excellent tracer of diesel exhaust. Additionally at the elevated locations, measurements of atmospheric wind and turbulence were made using three sonic anemometers. The SMPS instruments measure particle number concentrations size fractionated over the range from 17 to 600 nanometers diameter in 105 size bins (51 bins at North Kensington and Marylebone Road), and at the Regents University site this was supplemented by an additional SMPS with a nano-differential mobility analyser, measuring particle diameters down to 5 nanometers. Examples of the measured size distributions appear in Figure 6 which shows campaign-average particle number size distributions at Marylebone Road and Regents University and Figure S4 which shows weekday-weekend differences in particle size distributions at these sites. From Figure 6 it is seen that overall number concentrations (areas under the curves) diminish substantially from the roadside Marylebone Road site to the background Regent's University site in the park. However, one feature of the park site data not seen at other ground-level sampling sites is a loss of the large mode

at 20-30 nm seen in the Marylebone Road data and attributed primarily to the semi-volatile diesel particles, as well as an increase in the relative abundance of the <20 nm particles, consistent with evaporative shrinkage. As the Regent's University site was downwind of Marylebone Road for the vast majority of the campaign period, the influence of advected traffic particles is expected, and appears clearly in the data. Both the diurnal pattern of traffic flows and the vehicle mix change on Marylebone Road between weekdays and the weekend, and this is reflected in the average size distributions seen in Figure S4 for the Marylebone Road site. The main feature is the much lower magnitude of the 20-30 nm mode at weekends, which disappears almost entirely at the Regent's University site.

The particle size distributions (Figures 6 and S4) can be considered as the sum of a number (usually three) of log-normal modes, which can be fitted by an iterative algorithm to find for each mode an optimal mode diameter, first derivative of particle number ($dN/dlogD_p$) at the mode size, and mode width. Fitting in this manner reveals a nucleation mode at the Marylebone Road site centred on 20-25 nm diameter, which has reduced in size at Regent's University to be within the range of <20 nm. Earlier work using a site in the centre of Regent's Park, which is further than the current site from Marylebone Road, has shown shrinkage of this mode to below 10 nm [64]. The campaign data were used to calculate apparent particle shrinkage rates, using adjusted wind speed data from Heathrow airport to estimate travel times between the Marylebone Road and Regent's University sites. Oxidation of biogenic organic compounds can lead to new particle formation [65], but our earlier data analyses [64] discount this as affecting the particle size distributions. The average condensation sink for the Regent's Park aerosol (defined as a timescale for sulphuric acid vapour condensation) is 5.8 x $10^{-3}$ $s^{-1}$, implying a lifetime for the molecule of a few minutes. In contrast, the lifetimes of small particles with respect to scavenging by other particles are much longer, by a factor of almost 200 for 10 nm particles and over 2,000 for 40 nm particles.

The SVOC evaporation rate, and hence the particle shrinkage rate, is sensitive to the difference between the saturation vapour pressure at the particle surface for each particular SVOC and the partial pressure in the ambient air surrounding the particle. Consequently, air samples were collected using a filter to collect condensed phase material and an adsorption tube for vapour (see Supplementary Information), taking care to minimise post-collection particle to vapour phase transfer, with subsequent analysis of hydrocarbons using the GCxGC-ToFMS instrument. These measurements were made at the Westminster University and Regent's University sites, and additionally at Marylebone Road and Eltham, a background site in suburban south London. The latter sites measure $C_2$-$C_{10}$ vapour phase hydrocarbons routinely as part of a small national network of hydrocarbon measurements, allowing creation of an almost continuous dataset of simultaneously measured concentrations from $C_2$ to $C_{35}$. Figure 7 shows vapour and condensed phase concentrations of n- and iso-alkanes from $C_{12}$ to $C_{35}$ at the Eltham site, clearly exemplifying the large change in partitioning from vapour domination at $C_{12}$ to an almost wholly particulate composition at $C_{35}$. The broad similarity of the distributions seen at Eltham (Figure 7) to those in the diesel exhaust samples (Figure 4) strongly suggest that diesel emissions dominate the hydrocarbon composition of UK urban air in this molecular weight range.

**Science Topic 4: Street canyon and urban modelling**

The final component of this work is the construction of numerical models which simulate the behaviour of the semi-volatile particles between their emission and their sampling within a few kilometres of source. Kumar and coworkers [66] consider the scales and relevant factors for modelling nanoparticles from road traffic in the urban atmosphere, considering condensation, but not evaporation processes. Toenges-Schuller et al. [44] and Karl et al. [67] have both modelled traffic-generated particles in the urban areas, but include different processes in their models. Zhang and

Wexler [68] and Zhang et al. [69, 70] have established a theoretical framework for describing the behaviour of vehicle-emitted particles, developing a model which divides into separate "tailpipe to road" and "road to ambient" components. Both theoretical [71, 72] and experimental [73, 74] studies have sought to describe the "tailpipe to road", or initial few seconds of dilution. Wang and Zhang [75] and Wang et al. [76] have developed simulations of the "road to ambient" processes using a UFP model implemented in a CFD model with the RANS turbulence scheme. Our models use measured emission factors for particles and simulate the "road to ambient" processes up to neighbourhood scale (~ 1 km). We have utilised both a fluid-dynamically simple but microphysically complicated box model, which simulates the mean properties of particles in a street canyon and the evolution of the particles in a box of air as it moves away from the traffic, and a more fluid-dynamically complex Eulerian large-eddy simulation model with simpler microphysics, in which dominating turbulent eddies and their effects on mixing in the urban boundary layer are explicitly simulated within a 3-dimensional grid of boxes placed over central London. Such a combination of models allows us to investigate aerosol or turbulent mixing processes independently as well as together. We have also developed a model which simulates the effects of mixing upon the particle size distribution in a two-compartment street canyon [77], providing a framework for understanding how canyon geometry, street trees and furniture, and architectural features interact with the large-scale atmospheric flow to determine the properties of SVOC particles in street canyons.

A detailed description of the street canyon-neighbourhood CiTTyStreet-UFP model is given in Nikolova et al. [21]. The UFP aerosol module takes into account the multicomponent nature of the particles and can incorporate the relevant aerosol dynamic processes such as condensation/ evaporation, deposition and coagulation. The driving force for condensation/evaporation is the difference between the partial pressure of each representative Semi-Volatile Organic Compound (SVOC) and its saturation vapour pressure above the mixture. The condensation/evaporation rate is estimated from the relevant set of physical equations listed in the Supplementary Information. The

physical processes differ between larger particles (Dp ≫ mean free path, λ) and smaller particles ($D_P$ ≤ λ), with a transition regime between them described by the Fuchs-Sutugin correction term (see Supplementary Information). The fomulation used in this work derived from the former, continuum regime, although there is an alternative formulation based upon the physics of the latter, kinetic regime [78].

In our model configuration, we use surrogate n-alkanes in the range $C_{16}H_{34}$-$C_{32}H_{66}$ to represent 17 SVOC components with progressively lower volatilities; additionally, one component represents an involatile core. The use of surrogate n-alkanes allows us to use real physico-chemical data for vapour pressure, surface tension, and molecular volume. The full complexity of the diesel emissions and atmospheric measurements (Figure S2) are collapsed onto the surrogate n-alkanes by projecting the 2D chromatogram onto the volatility axis [60]. Nucleation and Aitken modes consist of 1% and 90% involatile core, respectively, based upon published data for the size of the involatile core [12, 13, 26]. While the difference between extremely low volatility SVOC and carbon/metal solid cores is not relevant in the modelling framework for the selected timescale (30 min), the human inflammatory response to organic or solid carbonaceous cores could be significant and has to be borne in mind [79, 80]. The model contains a gas phase chemistry module [81] but this was not extended to SVOC in the present work because the constituent residence times are much shorter than the e-folding times for reaction of even the most reactive SVOC with hydroxyl radical under ambient conditions [60].

Gas-phase SVOC concentrations are based on observational data next to a traffic site [82] and were used in the study of Nikolova et al. [21]. Saturation vapour pressure follows Compernolle et al. [83] as calculated by the UManSysProp online tool [61] which approximate well to our measured values, and accommodation coefficients followed Julin et al [84]. Table S1 presents the initial parameters related to particle composition, saturation vapour pressure, and partial pressures in the street canyon and above roof-top/background. The CiTTyStreet-UFP was run to steady state taking into account

emissions, exchange of UFP number and mass concentrations between the street canyon and the roof-top, mixing with background particulates, and condensation/evaporation. After a steady state is achieved, a further model simulation allows the roof-top particles to evolve subject to condensation/evaporation, using an 'ultrafine particle following' (Lagrangian) microphysics scheme for a timescale relevant for UFP transport in the neighbourhood scale (less than 1 km).

Figure 8 presents how the nucleation mode peak diameter $D_{pg,nuc}$ (= 23 nm) evolves with advection, from 0 seconds at the roof-top above the street canyon to 30 minutes downwind. From time *t*=0s to *t*=30 min, the initial $D_{pg,nuc}$ reduces by about 6 nm. The effective rate of diameter reduction is estimated following $(D_{pg,nuc,initial} - D_{pg,nuc,final})/t$, where $D_{pg,nuc,initial}$ is the initial diameter at time t=0s and $D_{pg,nuc,final}$ is the final diameter corresponding to time *t* [85]. We assume that as the particles with the peak diameter evaporate during the Lagrangian advection, the property of "peak diameter" is retained in the size distribution, i.e. the property is not shifted to other particles. Figure 9 shows that after 1 min of the advection, the particles lose about 45% of their original total mass of SVOC, i.e. $M_{pg,nuc,1min}/M_{pg,nuc,initial} \approx 0.55$. Considering that at the initial stage, nucleation and Aitken modes consist of 1% and 90% involatile core (IC), and this leads to about 20% of involatile core near the peak diameter. By including involatile core, the evaporation after 1 min yields a mass ratio of $R_{M,1min} = (M_{pg,nuc,1min} + M_{pg,nuc,IC})/(M_{pg,nuc,initial} + M_{pg,nuc,IC}) \approx 0.64$. This mass ratio gives the diameter at 1 min of $D_{pg,nuc,1min} = D_{pg,nuc,initial}\left(R_{M,1min}\right)^{1/3}$ because of the ratio of diameter is one-third power of the mass ratio. Noticing that $D_{pg,nuc,initial} \approx 23.1$ nm, we will have $D_{pg,nuc,1min} \approx 20$ nm, which is about the value shown in Figure 8. By applying the same principle to $t = 30$ min, $M_{pg,nuc,30min}/M_{pg,nuc,initial} \approx 0.31$ and $R_{M,30min} \approx 0.446$, which yields $D_{pg,nuc,initial} \approx 17.6$ nm, compared well with the value in Figure 8. The rapid decrease of the nucleation mode particles in the first 1 min is due to the evaporation of SVOC in the range $C_{16}H_{34}$-$C_{24}H_{52}$ as shown in Figure 9 where the overall mass per SVOC falls below 0.1 ng $m^{-3}$. The decrease in $D_{pg,nuc}$ after 1 min is promoted by the loss of mass from the higher molecular weight compounds

in the range of $C_{25}H_{52}$-$C_{29}H_{60}$. Marginal mass decreases of 0.34, 0.26 and 0.19 ng $m^{-3}$ are simulated for $C_{30}H_{62}$, $C_{31}H_{64}$ and $C_{32}H_{66}$, respectively, demonstrating that these components are effectively involatile over the modelled period.

Coagulation and deposition are found in our study to have a minor (1-5%) effect on the street-canyon UFP size distributions [21], although earlier work has attached more importance to these processes, albeit on greater distance scales [86]. Vapour pressure parameterisations have a very significant impact on particle size and composition [60], as do factors affecting the dispersion of air through a street canyon [77]. The UFP aerosol module is incorporated into the three-dimensional Large Eddy Simulation (LES) based on the Weather Research and Forecasting model (WRF) [87] to simulate the dispersion and evolution of nanoparticles at a neighbourhood-scale over central London. The WRF-LES model is a powerful atmospheric modelling system with large eddies explicitly calculated and small eddies parameterised by sub-grid scale turbulence schemes. The WRF-LES model handles the advection and diffusion of size-resolved multicomponent UFP tracers at the neighbourhood scale, while the UFP aerosol module solves microphysics (e.g. condensation/ evaporation processes) of multicomponent UFP.

The input sounding of WRF-LES can be derived based on the neighbourhood meteorological data (e.g. mixing layer height, temperature, and wind conditions). Traffic-induced UFP emissions from a gridded neighbourhood-scale street network over central London are incorporated into the WRF-LES model. An instantaneous snapshot of total UFP number concentration over central London under a southerly wind condition is shown in Figure 10 as an illustration. Traffic-generated UFPs vented out from an urban street network are transported by wind towards the north while they undergo the neighbourhood scale dispersion. This coupled WRF-LES-UFP model system can capture the behaviour of neighbourhood-scale UFP dispersion.

## CONCLUSIONS

This project was conceived following an unexpected observation of shrinkage of particles sampled in Regent's Park [64]. From a conceptual viewpoint, such shrinkage of diesel particles was to be expected but it had not been considered previously and such phenomena were not accounted for in the small number of available numerical models of traffic-related urban aerosol. This led to detailed studies in the engine laboratory to sample diesel exhaust particles under controlled conditions of engine operation, fuel and lubricant. Initially, the measurements were made on raw engine exhaust without any emissions abatement devices, but it was subsequently recognised that emissions abatement devices were becoming a major feature of the diesel vehicle fleet and their efficacy needed to be assessed. Consequently, the final measurement dataset incorporates not only the engine-out exhaust measurements but also evaluates the effect of a diesel oxidation catalyst and a diesel particulate filter. The inclusion of all three levels of technology is important because in many parts of the world the advanced control devices cannot be used because of an inadequate quality of fuel. Our results show clearly the inclusion of both unburnt diesel fuel and lubricating oil within the emitted particles and demonstrated that lubricant formulation significantly affected particle composition.

The complexity of the diesel samples created major challenges for the analytical laboratory but the availability of two-dimensional gas chromatography interfaced with Time-of-Flight Mass Spectrometry made a huge difference and allowed separation, characterisation and quantification of many hundreds of compounds. As the work progressed, we were able to modify the instrumentation to allow electron ionisation at lower energies hence leading to much lesser fragmentation of the ions allowing more confident characterisation of the compounds when used alongside the traditional 70 eV mass spectra. In this context, the work has provided information on both the condensed phase and vapour phase emissions from a diesel engine in previously unparalleled detail.

The field experiments threw up many challenges. Some of these were practical issues such as moving a major piece of equipment onto the roofs of buildings in central London with very limited access. However, the instruments, in the main, ran well and provided us with a very detailed dataset which upon analysis confirmed our earlier observations of particle shrinkage between Marylebone Road and the sampling site in Regent's Park. From this, we were able to calculate evaporation rates. We wanted to compare such rates with theoretical predictions but this required accurate knowledge of saturation vapour pressures of individual compounds which we had assumed would be available from the literature. However, although there were many datasets available in the literature, they differed for individual n-alkanes over a range of several orders of magnitude, necessitating the collection of new definitive data upon saturation vapour pressures. These were used to predict the rates of evaporation of hydrocarbons from complex mixtures and hence the rates of particle shrinkage.

All of the knowledge acquired in the engine laboratory, analytical laboratory, physico-chemical property studies and fieldwork were incorporated into numerical models using different descriptions of the atmosphere to simulate particle transport, mixing and evaporation on a spatial scale relevant to our observations in central London. This has led to a suite of numerical models which are able to take account of detailed particle microphysical processes in generating realistic information on particle numbers and size distributions at locations within central London.

Diesel particles are of considerable importance because of their dominance of the particle number in most urban atmospheres and their large contribution to a pollutant (particulate matter) with high human toxicity. However, when advected away from source into areas of lower vapour concentrations, so the semi-volatile constituents within the particles will have a strong tendency to evaporate, and this provides hydrocarbon vapour which will oxidise to form a larger mass of secondary organic aerosol which also contributes to the airborne concentration of toxic particulate matter. This has not been the subject of this research, but the data generated in terms of emission

factors, particle composition and physico-chemical properties are a valuable resource to numerical modellers wishing to simulate the formation of secondary organic aerosol within the atmosphere.

## DATA ACCESSIBILITY

Data supporting this publication are openly available from the UBIRA eData repository at https://doi.org/10.25500/eData.bham.00000265

## COMPETING INTERESTS

We have no competing interests.

## AUTHOR CONTRIBUTIONS

ARMK and XC led the modelling work which was conducted by IN and JZ; HX directed the engine laboratory where SZ-R operated the engine and collected samples, along with MSA and ZL. MSA, DCSB, ZL and RX carried out the field campaigns; MSA and CS ran the laboratory chemical analyses; data analyses were conducted by MSA, AS and RX; RMH conceived the study, designed the study, coordinated the study and prepared the first draft of the manuscript. All authors gave final approval for publication.

## ACKNOWLEDGEMENT

Financial support from the European Research Council (ERC-2012-AdG, Proposal No. 320821) for the FASTER project is gratefully acknowledged. The authors are also grateful to Westminster University, Regent's University, King's College, London and B.T. for access to sampling locations, and to King's College and Transport for London for traffic data. The authors thank James Brean for assistance with the fieldwork in London.

## FUNDING STATEMENT

Financial support was received from the European Research Council (ERC-2012-AdG, Proposal No. 320821).

## ETHICS STATEMENT

There are no ethical concerns relating to this research. This research was subject to ethical scrutiny by the University of Birmingham Research Ethics Committee and the European Research Executive Agency prior to commencement.

## REFERENCES

1. Cohen AJ, Brauer M, Burnett R, Anderson HR, Frostad J, Estep K, Balakrishnan K, Brunekreef B, Dandona L, Dandona R, Feigin V, Freedman G, Hubbell B, Jobling A, Kan H, Knibbs L, Liu Y, Martin R, Morawska L, Pope III CA, Shin H, Straif K, Shaddick G, Thomas M, van dingenen R, van Donkelaar A, Vos T, Murray CJL, Forousanfar MH. 2017 Estimates and 25-year trends of the global burden of disease attributable to ambient air pollution: an analysis of data from the Global Burden of Diseases Study 2015. *Lancet* **389**, 1907-1918. (doi: http://dx.doi.org/10.1016/S0140-6736(17)30505-6)

2. Shi JP, Xi S, Khan A, Mark D, Kinnersley R, Yin J. 2000 Measurement of number, mass and size distribution of particles in the atmosphere, R.M. Harrison. *Phil. Trans. R. Soc. Lond. A* **358**, 2567-2580. (doi: 10.1098/rsta.2000.0669)

3. Harrison RM, Yin J. 2000 Particulate matter in the atmosphere: Which particle properties are important for its effects on health? *Sci. Tot. Environ.* **249**, 85-101. (https://doi.org/10.1016/S0048-9697(99)00513-6)

4. Kelly FJ, Fussell JC. 2012 Size, source and chemical composition as determinants of toxicity attributable to ambient particulate matter. *Atmos. Environ.* **60**, 504-526. (http://dx.doi.org/10.1016/j.atmosenv.2012.06.039)

5. Kumar P, Morawska L, Birmili W, Paasonen P, Hu M, Kulmala M, Harrison RM, Norford L., Britter R. 2014 Ultrafine particles in cities. Environ. Intl. 66, 1-10.

(doi: 10.1016/j.envint.2014.01.013)

6. Beddows DCS, Harrison RM. 2008 Comparison of average particle number emission factors for heavy and light duty vehicles derived from rolling chassis dynamometer and field studies. *Atmos. Environ*. **42**, 7954-7966. (doi:10.1016/j.atmosenv.2008.06.021)

7. Atkinson RW, Fuller GW, Anderson HR, Harrison RM, Armstrong B. 2010 Urban ambient particle metrics and health: a time-series analysis. *Epidemiology*, **21**, No. 4, 501-511. (doi: 10.1097/EDE.0b013e3181debc88)

8. Reche C, Querol X, Alastuey A, Viana M, Pey J, Moreno T, Rodriguez S, Gonzalez Y, Fernandez-Camacho R, Sanchez de la Campa AM, de la Rosa J, Dall'Osto M, Prevot ASH, Hueglin C, Harrison RM, Quincey P. 2011 New considerations for PM, black carbon and particle number concentration for air quality monitoring across different European cities. *Atmos. Chem. Phys.* **11**, 6207-6227. (doi:10.5194/acp-11-6207-2011)

9. Beddows DCS, Harrison RM, Green D, Fuller G. 2015 Receptor modelling of both particle composition and size distribution data from a background site in London UK. *Atmos. Chem. Phys.* **15**, 10107-10125. (doi:10.5194/acp-15-10107-2015)

10. Shi JP, Harrison RM. 1999 Environ. Investigation of ultrafine particle formation during diesel exhaust dilution. *Sci. Technol*. **33**, 3730-3736. (doi: 10.1021/es981187l)

11. Charron A, Harrison RM. 2003 Primary particle formation from vehicle emissions during exhaust dilution in the roadside atmosphere. *Atmos. Environ.* **37,** 4109-4119. (doi: 10.1016/S1352-2310(03)00510-7)

12. Ronkko T, Virtanen A, Kannosto J, Keskinen J, Lappi M, Pirjola L. 2007 Nucleation mode particles with a nonvolatile core in the exhaust of a heavy duty diesel vehicle. *Environ. Sci. Technol.* **41**, 6384-6389. (doi: 10.1021/es0705339)

13. Kirchner U, Scheer V, Vogt R, Kagi R. 2009 TEM study on volatility and potential presence of solid cores in nucleation mode particles from diesel powered passenger cars. *Aerosol Sci.*, **40**, 55-64. (doi:10.1016/j.jaerosci.2008.08.002).

14. Shi JP, Mark D, Harrison RM. 2000 Characterization of particles from a current technology heavy-duty diesel engine. *Environ. Sci. Technol.* **34**, 748-755. (doi: 10.1021/es990530z)

15. Ristimaki J, Vaaraslahti K, Lappi M, Keskinen J. 2007 Hydrocarbon condensation in heavy-duty diesel exhaust. *Environ. Sci. Technol.* **41**, 6397-6402. (doi:10.1021/es0624319)

16. Olivares G, Johansson C, Strom J, Hansson, H-C. 2007 The role of ambient temperature for particle number concentrations in a street canyon. *Atmos. Environ.* **41**, 2145-2155. (doi.org/10.1016/j.atmosenv.2006.10.068)

17. Fujitani Y, Kumar P, Tamura K, Fushimi A, Hasegawa S, Takahashi K, Tanabe K, Kobayashi S, Hirano S. 2012 Seasonal differences of the atmospheric particle size distribution in a metropolitan area in Japan. *Sci. Tot. Environ.* **437**, 339-347. (doi.org/10.1016/j.scitotenv.2012.07.085)

18. Gramotnev G, Ristovski Z. 2004 Experimental investigation of ultra-fine particle size distribution near a busy road. *Atmos. Environ.*, **38**, 1767-1776. (doi:10.1016/j.atmosenv.2003.12.028)

19. Jeong C-H, Evans GJ, Healy RM, Jadidian P, Wentzell J, Liggio J, Brook JR. 2015 Rapid physical and chemical transformation of traffic–related atmospheric particles near a highway. *Atmos. Pollut. Res.* **6**, 662-672. (doi: 10.5094/APR.2015.075)

20. Choi W, Paulson SE. 2016 Closing the ultrafine particle number concentration budget at road-to-ambient scale: Implications for particle dynamics. *Aerosol Sci Technol.*, **50**, 448-461. (doi.org/10.1080/02786826.2016.1155104)

21. Nikolova I, MacKenzie AR, Cai X, Alam MS, Harrison RM. 2016 Modelling component evaporation and coposition change of traffic-induced ultrafine particles during travel from street canyon to urban background. *Faraday Discuss.* **189**, 529-546. (doi: 10.1039/c5fd00164a)

22. Seinfeld JH, Pandis SN. 2006 Atmospheric Chemistry and Physics: From Air Pollution to Climate Change, 2nd Revised edition. ISBN: 978-0-471-72018-8

23. Fushimi, A., Hasegawa, S., Takahashi, K., Fujitani, Y., Tanabe, K., Kobayashi, S. 2008 Atmospheric fate of nuclei-mode particles estimated from the number concentrations and chemical composition of particles measured at roadside and background sites. *Atmos. Environ.* **42**, 949-959. (doi:10.1016/j.atmosenv.2007.10.019)

24. Fernandez-Diaz JM, Rodriguez Brana MA, Arganza Garcia B, Gonzalez-Pola Muniz C, Garcia Nieto PJ. 1999 Difficulties inherent to the use of analytic solution of the condensation evaporation equation for multicomponent aerosols. *Atmos. Environ.* **33**, 1245-1259. (https://doi.org/10.1016/S1352-2310(98)00274-X)

25. Lowe D, MacKenzie AR, Nikiforakis N, Kettleborough J. 2003 A condensed-mass advection based model of liquid polar stratospheric clouds. *Atmos. Chem. Phys.* **3**, 29-38. (https://www.atmos-chem-phys.net/3/29/2003/)

26. Biswas S, Ntziachristos L, Moore KF, Sioutas C. 2007 Particle volatility in the vicinity of a freeway with heavy-duty diesel traffic. *Atmos. Environ.* **41**, 3479-3493. (doi:10.1016/j.atmosenv.2006.11.059)

27. Sakurai H, Tobias H, Park K, Zarling D, Docherty KS, Kittelson DB, McMurry PH, Ziemann PJ. 2003 On-line measurements of diesel nanoparticle composition and volatility. *Atmos. Environ.* **37**, 1199-1210. (doi:10.1016/S1352-2310(02)01017-8)

28. Karjalainen P, Ntziachristos L, Murtonen T, Wihersaari H, Simonen P, Myllari F, Nylund N-O, Keskinen J, Ronkko T. 2016 Heavy duty diesel exhaust particles during engine motoring formed by lube oil consumption. *Environ. Sci. Technol.* **50** 12504-12511. (doi:10.1021/acs.est.6b03284)

29. Al-Kindi S, Pope FD, Beddows DC, Bloss WJ, Harrison RM. 2016 Size dependent chemical ageing of oleic acid aerosol under dry and humidified conditions. *Atmos. Chem. Phys.* **16**, 15561-15579. (doi: 10.5194/acp-16-15561-2016)

30. Donahue NM, Robinson AL, Stanier CO, Pandis SN. 2013 Coupled partitioning, dilution, and chemical aging of semivolatile organics. *Environ. Sci. Technol.* **40**, 2635-2643. (doi: 10.1021/es052297c)

31. Dunmore RE, Hopkins JR, Lidster RT, Lee JD, Evans MJ, Rickard AR, Lewis AC, Hamilton JF. 2015 Diesel-related hydrocarbons can dominate gas phase reactive carbon in megacities. *Atmos. Chem. Phys.* **15**, 9983-9996. (doi:10.5194/acp-15-9983-2015)

32. Ots R, Young DE, Vieno M, Xu L, Dunmore RE, Allan JD, Coe H, Williams LR, Herndon SC, Ng NL, Hamilton JF, Bergstrom R, Di Marco C, Nemitz E, Mackenzie IA, Kuenen JJP, Green DC, Reis S, Heal MR. 2016 Simulating secondary organic aerosol from missing diesel-related intermediate-volatility organic compound emissions during the Clean Air for London (ClearfLo) campaign. *Atmos. Chem. Phys.* **16**, 645306473. (doi:10.5194/acp-16-6453-2016)

33. Gordon TD, Presto AA, Nguyen NT, Robertson WH, Na K, Sahay KN, Zhang M, Maddox C, Rieger P, Chattopadhyay S, Maldonado H, Maricq MM, Robinson AL. 2014 Secondary organic aerosol production from diesel vehicle exhaust: impact of aftertreatment, fuel chemistry and driving cycle. *Atmos. Chem. Phys.* **14**, 4643-4659. (doi.org/10.5194/acp-14-4643-2014)

34. Robinson AL, Donahue NM, Shrivastava MK, Weitkamp EA, Sage AM, Grieshop AP, Lane TE, Pierce JR, Pandis SM. 2007 Rethinking organic aerosols: Semivolatile emissions and photochemical aging. *Science* **315**, 1259-1262. (doi: 10.1126/science.1133061)

35. Presto AA, Miracolo MA, Kroll JH, Worsnop DR, Robinson AL, Donahue NM. 2009 Intermediate-volatility organic compounds: a potential source of ambient oxidized organic aerosol. *Environ. Sci. Technol.* **43**, 4744-4749. (doi: 10.1021/es803219q)

36. Zhao Y, Hennigan CJ, May AA, Tkacik DS, A. de Gouw J, Gilman JB, Kuster WC, Borbon A, Robinson AL. 2014 Intermediate-volatility organic compounds: a large source of secondary organic aerosol. *Environ. Sci. Technol.* **48**, 13743-13750. (dx.doi.org/10.1021/es5035188)

37. Gentner DR, Isaacman G, Worton DR, Chan AWH, Dallmann TR, Davis L, Liu S, Day DA, Russell LM, Wilson KR, Weber R, Guha A, Harley RA, Goldstein AH. 2012 Elucidating secondary organic aerosol from diesel and gasoline vehicles through detailed characterization of organic carbon emissions. *PNAS* **109**, 18318-18323. (doi:10. 1073/pnas.1212272109/-/DCSupplemental)

38. Gentner DR, Jathar SH, Gordon TD, Bahreini R, Day DA, El Haddad I, Hayes PL, Pieber SM, Platt SM, de Gouw J, Goldstein AH, Harley RA, Jimenez JL, Prevot ASH, Robinson AL. 2017 Review of urban secondary organic aerosol formation from gasoline and diesel motor vehicle emissions. *Environ. Sci. Technol.*, **51**, 1074-1093. (doi: 10.1021/acs.est.6b04509)

39. Perrone MG, Carbone C, Faedo D, Ferrero L, Maggioni A, Sangiorgi G, Bolzacchini E. 2014 Exhaust emissions of polycyclic aromatic hydrocarbons, n-alkanes and phenols from vehicles coming within different European classes. *Atmos. Environ.*, **82**, 391-400. (doi.org/10.1016/j.atmosenv.2013.10.040)

40. Schauer JJ, Kleeman MJ, Cass GR, Simoneit BRT. 1999 Measurement of emissions from air pollution sources. 2. C1 through C30 organic compounds from medium duty diesel trucks. *Environ. Sci. Technol.*, **33**, 1578-1587. (doi: 10.1021/es980081n)

41. Kittelson DB, Watts WF, Johnson JP. 2006 On-road and laboratory evaluation of combustion aerosols—Part 1: Summary of diesel engine results. *J. Aerosol Sci.* **37**, 913-930. (doi.org/10.1016/j.jaerosci.2005.08.005)

42. Kittelson DB, Watts WF, Johnson JP, Rowntree C, Payne M, Goodier S, Warrens C, Preston H, Zink U, Ortiz M, Goersmann C, Twigg MV, Walker AP, Caldow R. 2006 On-road evaluation of two Diesel exhaust aftertreatment devices. *J. Aerosol Sci.* **37**, 1140-1151. (doi:10.1016/j.jaerosci.2005.11.003)

43. Alam MS, Zeraati-Rezaei SZ, Stark CP, Liang Z, Xu HM, Harrison RM. 2016 The characterisation of diesel exhaust particles – composition, size distribution and partitioning. *Faraday Discuss.* **189**, 69-84. (doi: 10.1039/c5fd00185d)

44. Toenges-Schuller N, Schneider Chr, Niederau A, Vogt R, Birmili W. 2015 Modelling particle number concentrations in a typical street canyon in Germany and analysis of future trends. *Atmos. Environ*. **111**, 127-135. (doi.org/10.1016/j.atmosenv.2015.04.006)

45. Guan B, Zhan R, Lin H, Huang Z. 2015 Review of the state-of-the-art of exhaust particulate filter technology in internal combustion engines. *J. Environ. Manage.* **154**, 225-258. (doi.org/10.1016/j.jenvman.2015.02.027)

46. Lipsky EM, Robinson AL. 2006 Effects of dilution on fine particle mass and partitioning of semivolatile organics in diesel exhaust and wood smoke. *Environ. Sci. Technol.* **40**, 155-162. (doi: 10.1021/es050319p)

47. Kim Y, Sartelet K, Seigneur C, Charron A, Besombes J-L, Jaffrezo J-L, Marchand N, Polo. 2016 Effect of measurement protocol on organic aerosol measurements of exhaust emissions from gasoline and diesel vehicles. *Atmos. Environ.*, **140**, 176-187. (doi.org/10.1016/j.atmosenv.2016.05.045)

48. Fujitani Y, Saitoh K, Fushimi A, Takahashi K, Hasegawa S, Tanabe K, Kobayashi S, Furuyama A, Hirano S, Takami A. 2012 Effect of isothermal dilution on emission factors of organic carbon and n-alkanes in the particle and gas phases of diesel exhaust. *Atmos. Environ.* **59**, 389-397. (doi.org/10.1016/j.atmosenv.2012.06.010)

49. Alam M., Harrison RM. 2016 Recent advances in the application of 2-dimensional gas chromatography with soft and hard ionisation time-of-flight mass spectrometry in environmental analysis. *Chem. Sci.* **7**, 3968-3977. (doi: 10.1039/c6sc00465b)

50. Alam MS, Stark C, Harrison RM. 2016 Using variable ionisation energy time-of-flight mass spectrometry with comprehensive GC×GC to identify isomeric species. *Anal. Chem.* **88**, 4211-4220. (doi: 10.1021/acs.analchem.5b03122)

51. Alam MS, Liang Z, Zeraati-Rezaei S, Stark C, Xu H, MacKenzie AR, Harrison RM. 2018 Mapping and quantifying isomer sets of hydrocarbons (≥C12) in diesel exhaust, lubricating oil and diesel fuel samples using GC×GC-ToFMS. *Atmos. Meas. Tech*. **11**, 3047-3058. (doi.org/10.5194/amt-11-3047-2018)

52. Liang Z, Alam MS, Zeraati Rezaei S, Stark C, Xu H, Harrison RM. 2018 Comprehensive chemical characterization of lubricating oils used in modern vehicular engines utilizing GC×GC-TOFMS. *Fuel* **220**, 792-799. (doi.org/10.1016/j.fuel.2017.11.142)

53. Kleeman MJ, Riddle SG, Robert MA, Jakober CA. 2008 Lubricating Oil and Fuel Contributions To Particulate Matter Emissions from Light-Duty Gasoline and Heavy-Duty Diesel Vehicles. *Environ. Sci. Technol.*, **42**, 235-242. (doi: 10.1021/es071054c)

54. Fushimi A, Saitoh K, Fujitani Y, Hasegawa S, Takahashi K. 2011 Organic-rich nanoparticles (diameter: 10-30 nm) in diesel exhaust: Fuel and oil contribution based on chemical composition. *Atmos. Environ.* **35**, 6326-6336. (doi.org/10.1016/j.atmosenv.2011.08.053)

55. Harrison RM, Beddows DCS, Dall'Osto M. 2011 PMF analysis of wide-range particle size spectra collected on a major highway. *Environ. Sci. Technol*. **45**, 5522-5528. (dx.doi.org/10.1021/es2006622)

56. Vaaraslahti K, Virtanen A, Ristimaki J, Keskinen J. 2004 Nucleation mode formation in heavy-duty diesel exhaust with and without a particulate filter. *Environ. Sci. Technol.* **38**, 4884-4890. (doi: 10.1021/es0353255)

57. Vaaraslahti K, Keskinen J, Giechaskiel B, Solla A, Murtonen T, Vesala H. 2005 Effect of lubricant on the formation of heavy-duty diesel exhaust nanoparticles. *Environ. Sci. Technol.*, **39**, 8497-8504. (doi: 10.1021/es0505503)

58. Leblanc M, Noël L, R'Mili B, Boréave A, D'Anna B, Raux S. 2016 Impact of engine warm-up and DPF active regeneration on regulated and unregulated emissions of a Euro 6 diesel SCR equipped vehicle. *J. Earth Sci. Geotechn. Engineer.* **6**, 29-50.

59. R'Mili B, Boreave A, Meme A, Vernoux P, Leblanc M, Noel L, Raux S, D'Anna B. 2018 Physico-chemical characterization of fine and ultrafine particles emitted during diesel particulate filter active regeneration of Euro5 diesel vehicles. *Environ. Sci. Technol.* **52**, 3312-3319. (doi:10.1021/acs.est.7b06644)

60. Nikolova I, Cai X, Alam MS, Zeraati-Rezaei S, Zhong J, MacKenzie AR, Harrison RM. 2017 The influence of particle composition upon the evolution of urban ultrafine diesel particles on the neighbourhood scale. *Atmos. Chem. Phys. Discuss.* accepted. (https://doi.org/10.5194/acp-2017-1018)

61. Topping D, Barley M, Bane MK, Higham N, Aumont B, Dingle N, McFiggans G. 2016 UManSysProp v1.0: an online and open-source facility for molecular property prediction and atmospheric aerosol calculations. *Geosci. Model Dev.* **9**, 899-914. (doi: 10.5194/gmd-9-899-2016)

62. Verevkin SP, Wandschneider D, Heintz A. 2000 Determination of vaporization enthalpies of selected linear and branched $C_7$, $C_8$, $C_{11}$, and $C_{12}$ monoolefin hydrocarbons from transpiration and correlation gas-chromatography methods. *J. Chem. Eng. Data* **45**, 816-625. (doi: 10.1021/je990297k)

63. Harrison RM, Jones AM, Beddows DCS, Dall'Osto M, Nikolova I. 2016 Evaporation of traffic-generated nanoparticles during advection from source. *Atmos. Environ.* **125**, 1-7. (http://dx.doi.org/10.1016/j.atmosenv.2015.10.077)

64. Dall'Osto M, Thorpe A, Beddows DCS, Harrison RM, Barlow JF, Dunbar T, Williams PI, Coe H. 2011 Remarkable dynamics of nanoparticles in the urban atmosphere. *Atmos. Chem. Phys.* **11**, 6623-6637. (doi:10.5194/acp-11-6623-2011)

65. Riccobono F, Schobesberger S, Scott CE, Dommen J, Ortega IK, Rondo L, Almeida J, Amorim A, Bianchi F, Breitenlechner M, David A, Downard A, Dunne EM, Duplissy J, Ehrhart S, Flagan RC, Franchin A, Hansel A, Junninen H, Kajos M, Keskinen H, Kupc A, Kürten A, Kvashin AN, Laaksonen A, Lehtipalo K, Makhmutov V, Mathot S, Nieminen T, Onnela A, Petäjä T, Praplan AP, Santos FD, Schallhart S, Seinfeld JH, Sipilä M, Spracklen DV, Stozhkov Y, Stratmann F, Tomé A, Tsagkogeorgas G, Vaattovaara P, Viisanen Y, Vrtala A, Wagner PE, Weingartner E, Wex H, Wimmer D, Carslaw KS, Curtius J, Donahue NM, Kirkby J, Kulmala M, Worsnop DR, Baltensperger U. 2014 Oxidation products of biogenic emissions contribute to nucleation of atmospheric particles. *Science* **344**, 717-721. (doi: 10.1126/science.1243527)

66. Kumar P, Ketzel M, Vardoulakis S, Pirjola L, Britter R. 2011 Dynamics and dispersion modelling of nanoparticles from road traffic in the urban atmospheric environment - A review. *J. Aerosol Sci.* **42**, 580-603. (doi:10.1016/j.jaerosci.2011.06.001)

67. Karl M, Kukkonen J, Keuken MP, Lutzenkirchen S, Pirjola L, Hussein T. 2016 Modeling and measurements of urban aerosol processes on the neighborhood scale in Rotterdam, Oslo and Helsinki. *Atmos. Chem. Phys.* **16**, 4817-4835. (doi.org/10.5194/acp-16-4817-2016)

68. Zhang KM, Wexler AS. 2004 Evolution of particle number distribution near roadways-Part I: analysis of aerosol dynamics and its implications for engine emission measurement. *Atmos. Environ.* **38**, 6643-6653. (doi:10.1016/j.atmosenv.2004.06.043)

69. Zhang KM, Wexler AS, Zhu YF, Hinds WC, Sioutas C. 2004 Evolution of particle number distribution near roadways. Part II: the 'Road-to-Ambient' process. *Atmos. Environ.* **38**, 6655-6665. (doi:10.1016/j.atmosenv.2004.06.044)

70. Zhang KM, Wexler AS, Niemeier DA, Zhu Y, Hinds WC, Sioutase C. 2005 Evolution of particle number distribution near roadways. Part III: Traffic analysis and on-road size resolved particulate emission factors. *Atmos. Environ.* **39**, 4155-4166. (doi:10.1016/j.atmosenv.2005.04.003)

71. Lemmetty M, Pirjola L, Makelaa JM, Ronkkoa T, Keskinen J. 2006 Computation of maximum rate of water–sulphuric acid nucleation in diesel exhaust. *Aerosol Sci.* **37**, 1596-1604. (doi:10.1016/j.jaerosci.2006.04.003)

72. Vouitsis E, Ntziachristos L, Samaras Z. 2005 Modelling of diesel exhaust aerosol during laboratory sampling. *Atmos. Environ*. **39**, 1335-1345. (doi:10.1016/j.atmosenv.2004.11.011)

73. Ning Z, Cheung CS, Liu SX. 2004 Experimental investigation of the effect of exhaust gas cooling on diesel particulate. *Aerosol Sci.*, **35**, 333-345. (doi:10.1016/j.jaerosci.2003.10.001)

74. Ronkko T, Virtanen A, Vaaraslahti K, Keskinena J, Pirjola L, Lappic M. 2006 Effect of dilution conditions and driving parameters on nucleation mode particles in diesel exhaust: Laboratory and on-road study. *Atmos. Environ.*, **40**, 2893-2901. (doi:10.1016/j.atmosenv.2006.01.002)

75. Wang YJ, Zhang KM. 2012 Coupled turbulence and aerosol dynamics modeling of vehicle exhaust plumes using the *CTAG* model. *Atmos. Environ*. **59**, 284-298. (doi:10.1016/j.atmosenv.2012.04.062)

76. Wang YJ, Nguyen MT, Steffens JT, Tong Z, Wang Y, Hopke PK, Zhang KM. 2013 Modeling multi-scale aerosol dynamics and micro-environmental air quality near a large highway

intersection using the *CTAG* model. *Sci. Tot. Environ.* **443**, 375-386. (doi.org/10.1016/j.scitotenv.2012.10.102)

77. Zhong J, Nikolova I, Cai X, MacKenzie AR, Harrison RM. 2018 Modelling traffic-induced multicomponent ultrafine particles in urban street canyon compartments: Factors that inhibit mixing. *Environ. Pollut.* **238**, 186-195. (doi.org/10.1016/j.envpol.2018.03.002)

78. Tröstl J, Chuang WK, Gordon H, Heinritzi M, Yan C, Molteni U, Ahlm L , Frege C, Bianchi F, Wagner R, Simon M, Lehtipalo K, Williamson C, Craven JS, Duplissy J, Adamov A , Almeida J , Bernhammer A-K, Breitenlechner M, Brilke S, Dias A, Ehrhart S, Flagan RC, Franchin A, Fuchs C, Guida R, Gysel M, Hansel A, Hoyle CR, Jokinen T, Junninen H, Kangasluoma J, Keskinen H, Kim J, Krapf M, Kürten A, Laaksonen A, Lawler M, Leiminger M, Mathot S, Möhler O, Nieminen T, Onnela A, Petäjä T, Piel FM, Miettinen P, Rissanen MP, Rondo L, Sarnela N, Schobesberger S, Sengupta K, Sipilä M, Smith JN, Steiner G, Tomè A, Virtanen A, Wagner AC, Weingartner E, Wimmer D, Winkler PM, Ye P, Carslaw KS, Curtius J, Dommen J, Kirkby J, Kulmala M, Riipinen I, Worsnop DR, Donahue NM, Baltensperger U. 2016. The role of low-valatility organic compounds in initial particle growth in the atmosphere. *Nature* **533**, 527-531. (doi: 10.1038/nature18271)

79. Li R, Ning Z, Majumdar R, Cui J, Takabe W, Jen N, Sioutas C, Hsiai T. 2010 Ultrafine particles from diesel vehicle emissions at different driving cycles induce differential vascular pro-inflamatory responses: implications of chemical components and NF-kB signaling. *Part. Fibre Toxicol.* 7, **6**. (doi: doi:10.1186/1743-8977-7-6)
80. Xia M, Viera-Hutchins L, Garcia-Lloret M, Rivas MN, Wise P, McGhee S., Chatila ZK, Daher N, Sioutas C, Chatila, TA. 2015 Vehicular exhaust particles promote allergic airway inflammation through an aryl hydrocarbon receptor-notch signaling cascade. *J. Allergy Clin. Immun.* **136**, 441-453. (doi.org/10.1016/j.jaci.2015.02.014)

81. Pugh TAM, Cain M, Methven J, Wild O, Arnold SR, Real E, Law KS, Emmerson KM, Owen SM, Pyle JA, Hewitt CN, MacKenzie AR. 2012 A Lagrangian model of air-mass photochemistry and mixing using a trajectory ensemble: the Cambridge Tropospheric Trajectory model of Chemistry And Transport (CiTTyCAT) version 4.2. *Geosci. Model Dev.* **5**, 193-221. (doi:10.5194/gmd-5-193-2012)

82. Harrad S, Hassoun S, Callen Romero MS, Harrison RM. 2003 Characterisation and source attribution of the semi-volatile organic content of atmospheric particles and associate vapour phase in Birmingham, UK. *Atmos. Environ.* **37**, 4985-4991. (doi:10.1016/j.atmosenv.2003.07.012)

83. Compernolle S, Ceulemans K, Muller J-F. 2011 Evaporation: a new vapour pressure estimation method for organic molecules including non-additivity and intramolecular interactions. *Atmos. Chem. Phys.* **11**, 9431-9450. (doi: 10.5194/acp-11-9431-2011)

84. Julin J, Winkler PM, Donahue NM, Wagner PE, Riipinen I. 2014 Near-unity mass accomodation coefficient of organic molecules of varying structure. *Environ. Sci. Technol.* **48**, 12083-12089. (doi: 10.1021/es501816h)

85. Huang L, Gong SL, Gordon M, Liggio J, Staebier R, Stroud CA, Lu G, Mihele C, Brook JR, Jia CQ. 2014 Aerosol-computational fluid dynamics modeling of ultrafine and black carbon particle emission, dilution, and growth near roadways. *Atmos. Chem. Phys.* **14**, 12631-12648. (doi:10.5194/acp-14-12631-2014)

86. Gidhagen L, Johansson C., Langner J, Foltescu VL. 2005 Urban scale modeling of particle number concentration in Stockholm. *Atmos. Environ.* **39** 1711-1725. (doi:10.1016/j.atmosenv.2004.11.042)

87. WRF. 2018 Weather Research and Forecasting Model, National Centre for Atmospheric Research, Mesoscale and Microscale Meteorology Laboratory, Boulder, CO 80301, USA. (https://www.mmm.ucar.edu/weather-research-and-forecasting-model

## TABLE LEGENDS

**Table 1:** Groups of compounds analysed in the exhaust and atmospheric samples.

## FIGURE LEGENDS

**Figure 1:** Inter-connection of the main areas of research on airborne particulate matter.

**Figure 2:** Major processes affecting semi-volatile components of engine exhaust.

**Figure 3:** Science topics and objectives of the FASTER project.

**Figure 4:** A typical profile of n- + iso-alkane concentrations in the particulate and vapour phases from diesel engine exhaust emissions. Data from the test bed shown in Figure S1, running with ultra-low sulphur diesel fuel and fully synthetic motor oil. The sample was collected before DOC at low engine speed (1000 RPM) and low engine load (1.4 bar brake mean effective pressure).

**Figure 5:** Particle size distribution per kg of the fuel consumed before the diesel oxidation catalyst (DOC), after DOC and after the diesel particulate filter (DPF) at 1.4 bar brake mean effective pressure (BMEP) and 1800 revolutions per minute (RPM).

**Figure 6:** Overall mean particle size distribution at (a) Marylebone Road and (b) Regent's University using 2017 campaign data between 27$^{th}$ January and 16$^{th}$ February. Shaded area shows the standard deviation.

**Figure 7:** A typical profile of n- + iso-alkane concentration in the particulate and vapour phase from London Eltham.

**Figure 8:** Nucleation mode peak diameter evolution due to evaporation during advection from the roof-top for a timescale of 30 min.

**Figure 9:** Evolution of nucleation mode peak mass Mpg,nuc per (ng m$^{-3}$) per alkane from $C_{16}$ to $C_{32}$, presented for time 0 (initial), 1 and 30 min.

**Figure 10:** An instantaneous snapshot in the neighbourhood-scale dispersion of total UFP number concentration (# cm$^{-3}$; right hand scale) over central London with a southerly wind derived from the WRF-LES model.

**Table 1:** Groups of compounds analysed in the exhaust and atmospheric samples.

| |
|---|
| Linear and branched Alkanes (C12 – C35) |
| Monocyclic Alkanes (C12 – C33) |
| Bicyclic Alkanes (C12 – C33) |
| Tricyclic Alkanes (C12 – C33) |
| Monocyclic Aromatics (C12 – C33) |
| Bicyclic Aromatics (C12 – C33) |
| Aldehydes+Ketones (C9 – C30) |
| 16 PAHs |
| Alkyl naphthalenes (C11 – C16) |
| Biphenyls (Alkyl chain length C1 – C3) |
| Alkyl FLU/ANT/PHE (alkyl chain length C1 – C3) |

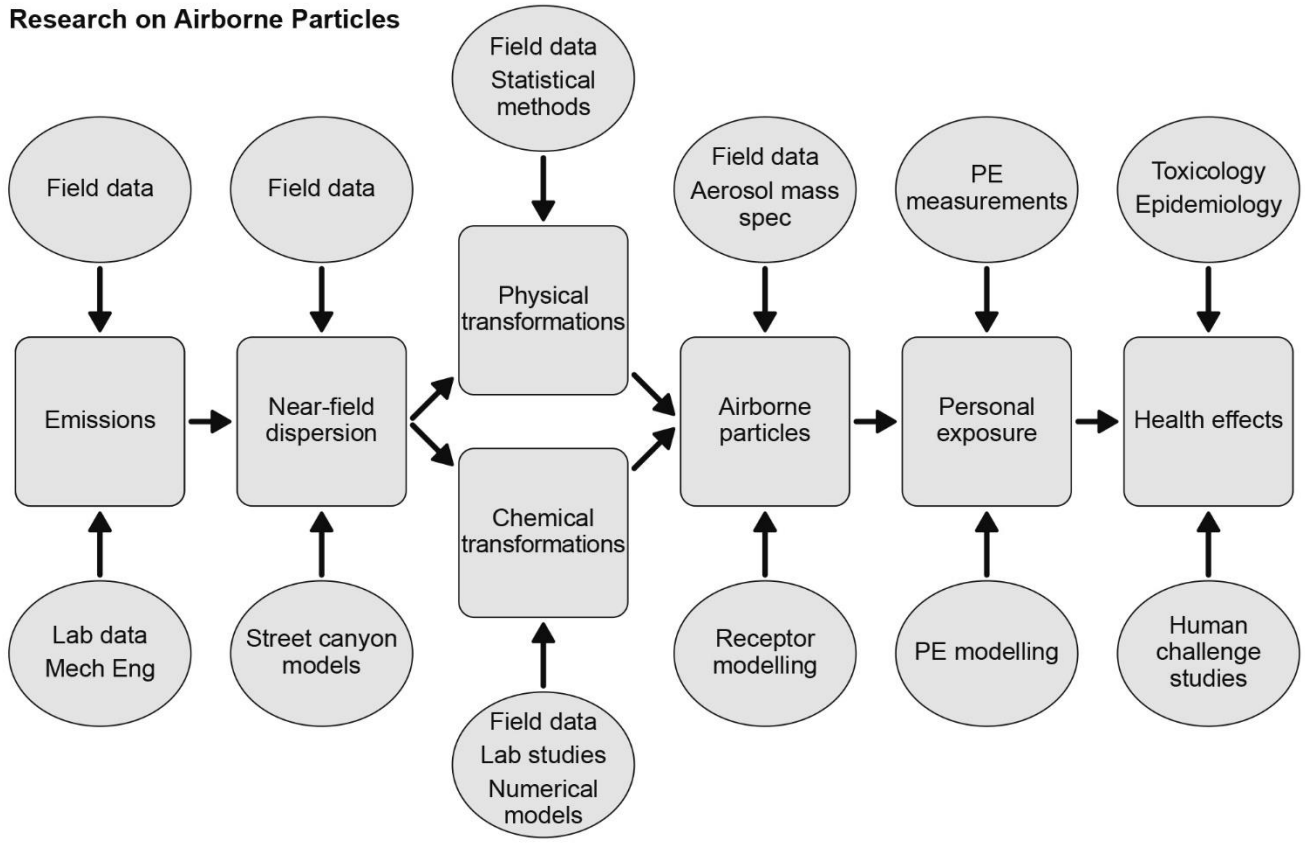


**Figure 1:** Inter-connection of the main areas of research on airborne particulate matter.

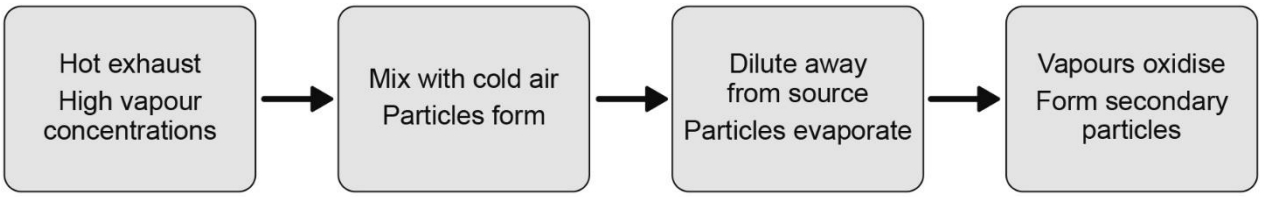


**Figure 2:** Major processes affecting semi-volatile components of engine exhaust.

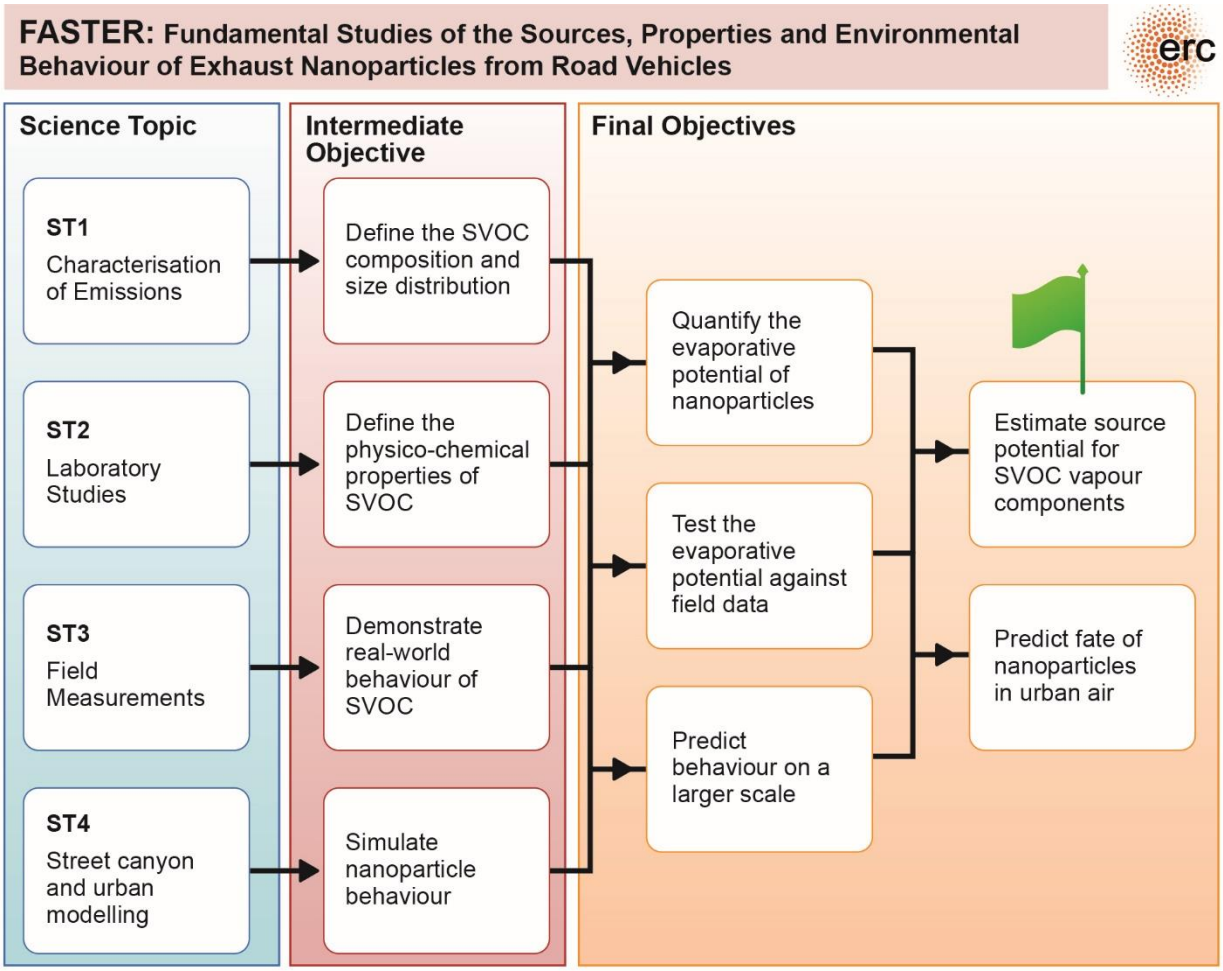


**Figure 3:** Science topics and objectives of the FASTER project.

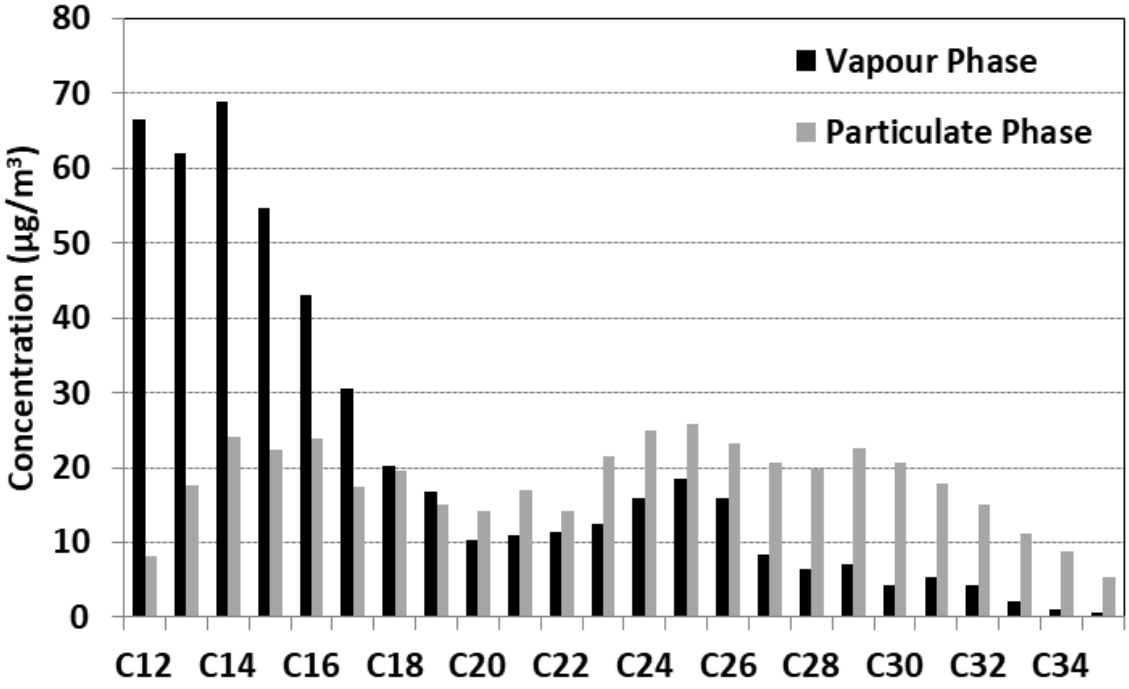


**Figure 4:** A typical profile of n- + iso-alkane concentrations in the particulate and vapour phases from diesel engine exhaust emissions. Data from the test bed shown in Figure S1, running with ultra-low sulphur diesel fuel and fully synthetic motor oil. The sample was collected before DOC at low engine speed (1000 RPM) and low engine load (1.4 bar brake mean effective pressure).

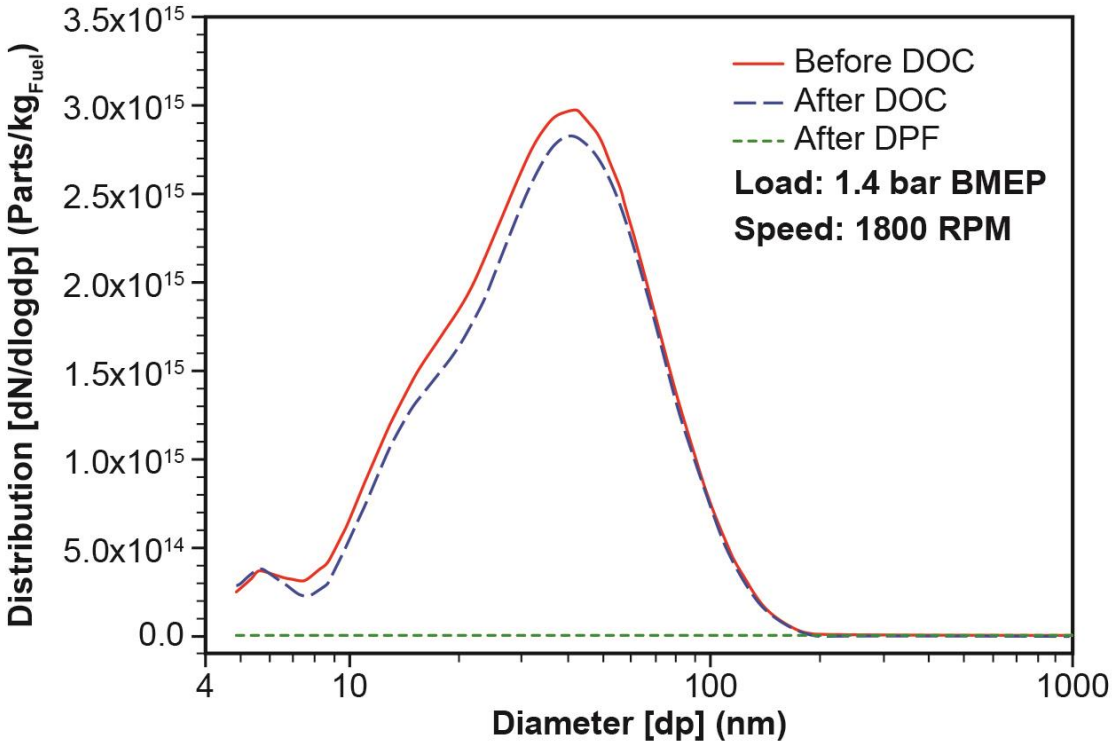


**Figure 5:** Particle size distribution per kg of the fuel consumed before the diesel oxidation catalyst (DOC), after DOC and after the diesel particulate filter (DPF) at 1.4 bar brake mean effective pressure (BMEP) and 1800 revolutions per minute (RPM).

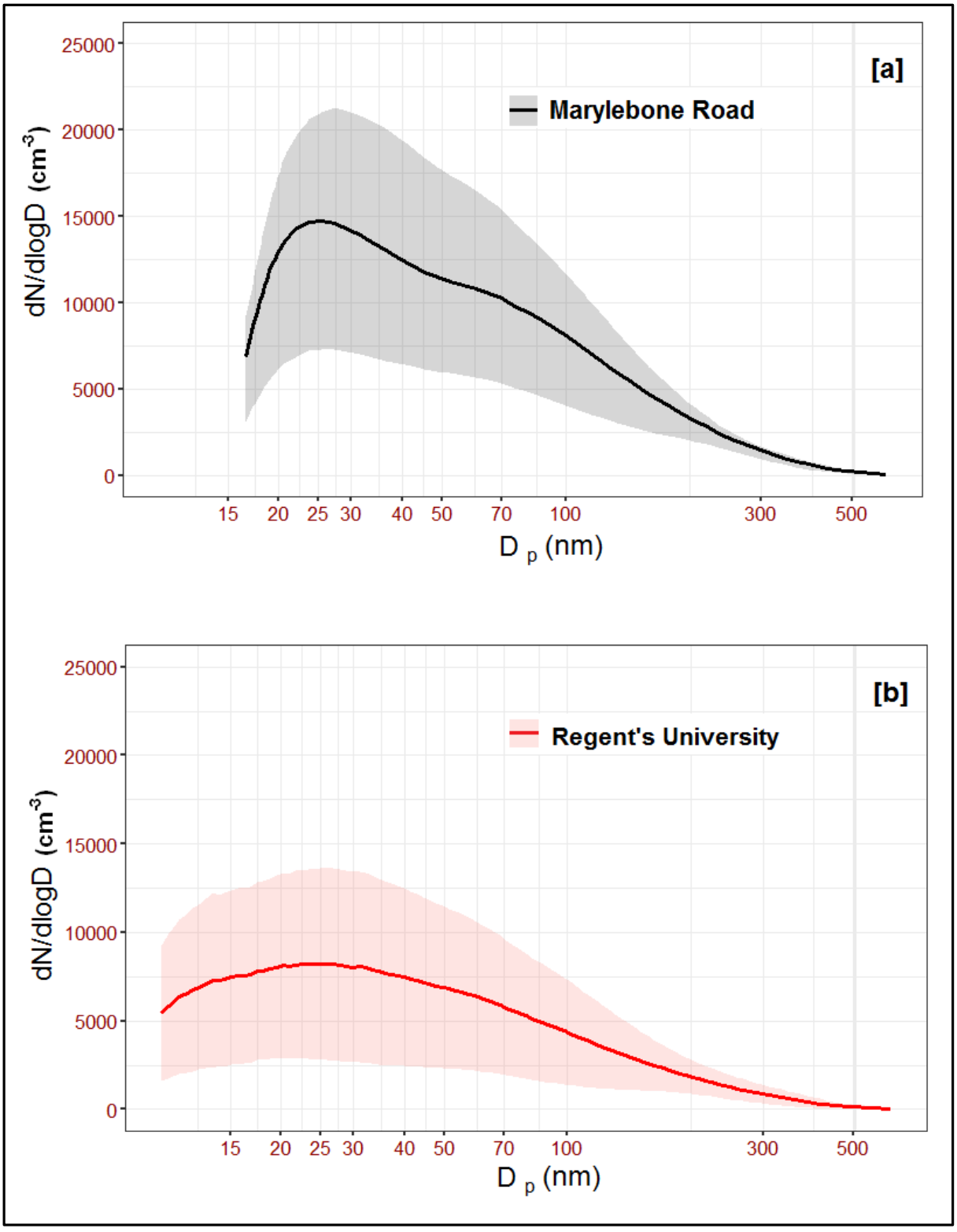


**Figure 6:** Overall mean particle size distribution at (a) Marylebone Road and (b) Regent's University using 2017 campaign data between 27th January to 16th February. Shaded area shows the standard deviation.

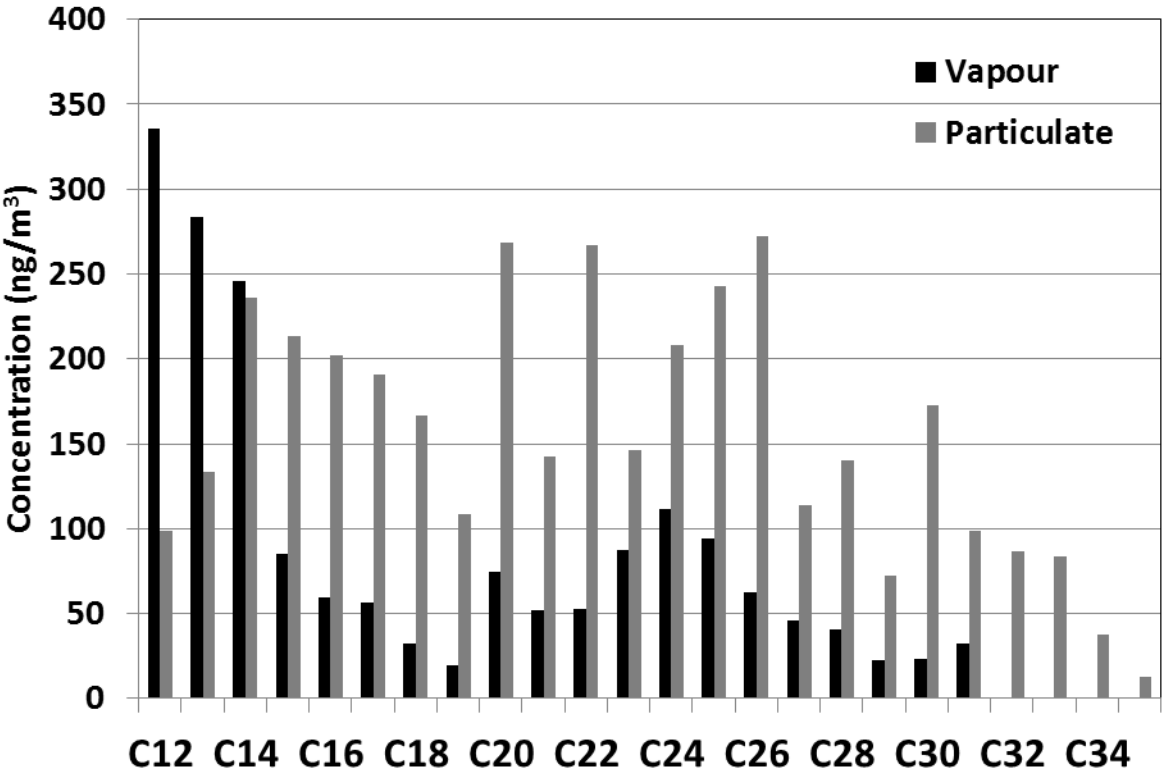


**Figure 7:** A typical profile of n- + iso-alkane concentration in the particulate and vapour phase from London Eltham.

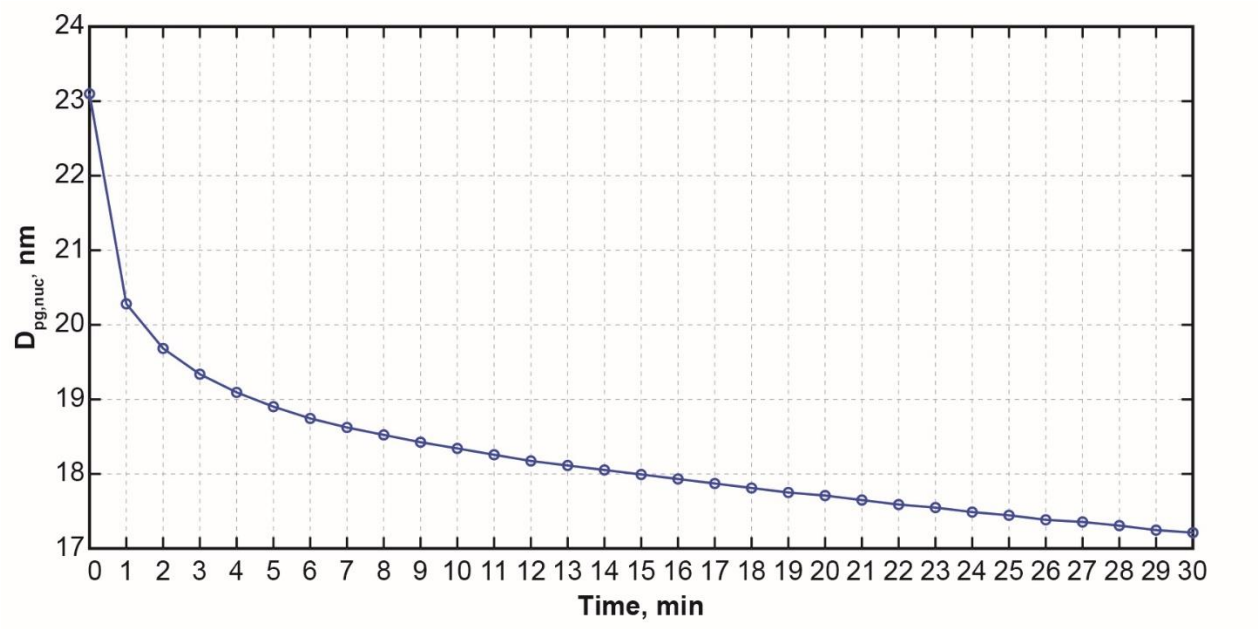


**Figure 8:** Nucleation mode peak diameter evolution due to evaporation during advection from the roof-top for a timescale of 30 min.

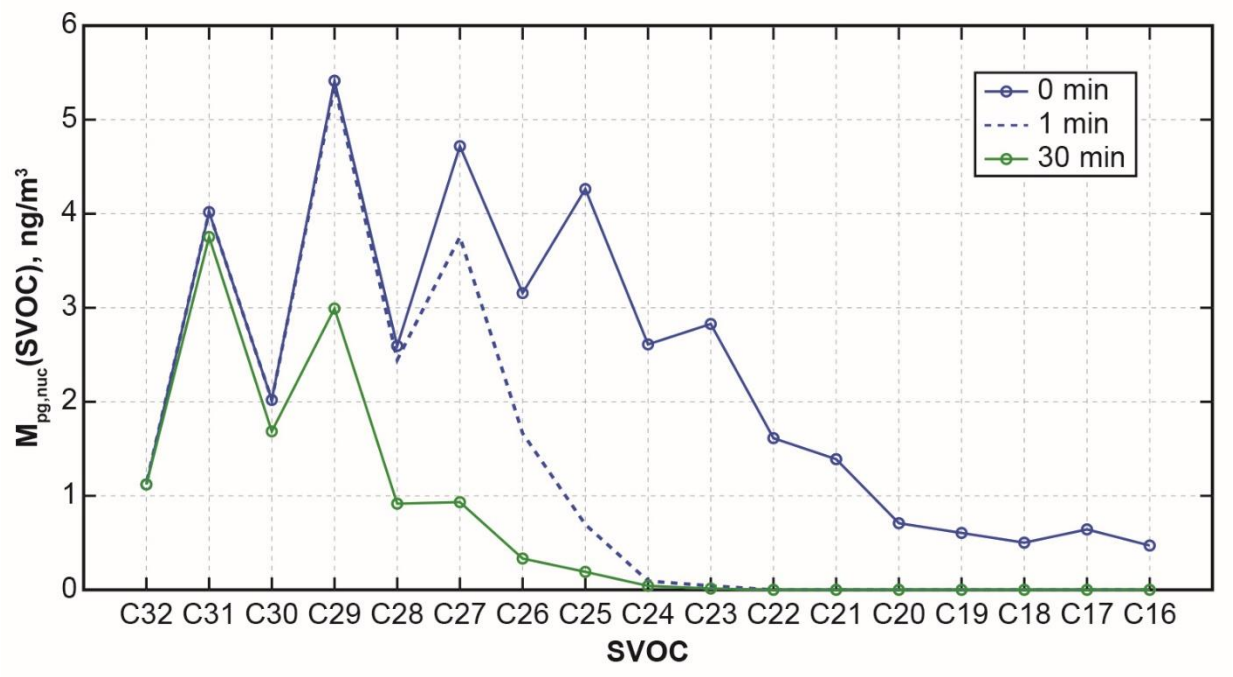


**Figure 9:** Evolution of nucleation mode peak mass Mpg,nuc per (ng $m^{-3}$) per alkane from $C_{16}$ to $C_{32}$, presented for time 0 (initial), 1 and 30 min.

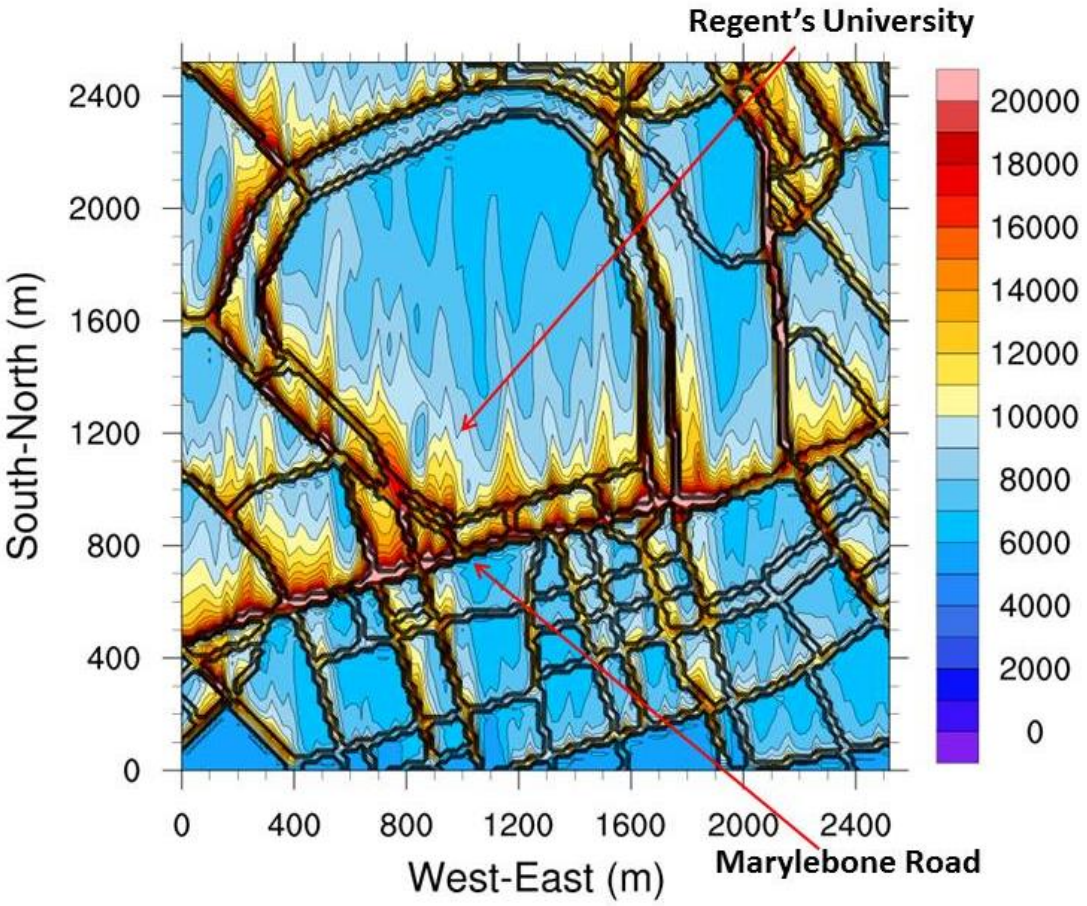


**Figure 10:** An instantaneous snapshot in the neighbourhood-scale dispersion of total UFP number concentration (# $cm^{-3}$; right hand scale) over central London with a southerly wind derived from the WRF-LES model.